Extended time–temperature rheology of polyvinyl butyral (PVB)

Carlos Arauz Moreno, Keyvan Piroird, Elise Lorenceau

Extended time–temperature rheology of polyvinyl butyral (PVB)

Carlos Arauz Moreno[1,2] · Keyvan Piroird[2] · Elise Lorenceau[1]

[1] Univ. Grenoble Alpes, CNRS, LIPhy, Grenoble 38000, France
[2] Saint-Gobain Research Paris, 39 Quai Lucien Lefranc, Aubervilliers 93360, France

Abstract

Polyvinyl butyral (PVB), used in safety glass and photovoltaic panels, is commonly described as a complex viscoelastic solid. However, this description is questionable: a viscoelastic solid rheology does not account well for the data obtained at high temperature and the value of the long-time elastic modulus is poorly defined. In this article, an extended rheological study of this polymer in shear geometry has been performed for temperatures ranging between 25°C to 140°C thanks to relaxation and oscillatory experiments. We provide the time-temperature superposition master curve for PVB as well as its time-temperature state diagram. Last, by interconverting the frequency measurements in the time scale and shifting the relaxation modulus through temperature-time superposition, we obtain the evolution of the relaxation modulus as a function of time over 13 orders of magnitude. This curve, well fitted by a generalized Maxwell model with only 10 Maxwell elements, reveals the predominance of the viscous character of PVB at long times with a vanishing long-term elastic modulus.

Keywords: Time-Temperature superposition, Polymer, long-term elastic moduli

1. Introduction

Polyvinyl butyral (PVB) is an amorphous polymer customarily found in stacked layered assemblies, such as safety glass (SG) and photovoltaic (PV) modules. In both implementations, the application or occurrence of high temperatures for prolonged periods of time appears to be a staple of the PVB life cycle. For instance, in both SG/PV modules, the PVB interlayer is processed roughly in the same manner by lamination of the full assembly inside autoclaves at high pressures and elevated temperatures (e.g., 135◦C) [1]. Similarly, in safety glass, PVB may be subjected to temperatures of 100°C for 16 hrs when the assembly undergoes so-called "bake" testing (see Norm EN ISO 12543-4). Meanwhile, PV modules may be "aged" at 85°C, under a moist atmosphere (relative humidity of 85%), for 1,000 hrs [2, 3]. Under these harsh conditions, both safety glass and PV modules may develop unwanted bubbles, blisters, finger instabilities, or even suffer delamination. These defects will develop all the more easily if the viscous character of the polymer dominates over its elastic character, hence the importance of knowing the rheology of PVB at elevated temperatures and long timescales.

A survey of the literature reveals that PVB has typically been studied under tension for temperature conditions and timescales relevant for glass performance during impact, bending, or breakage using Dynamical Mechanical Analysis (DMA) (Refs. [4, 5, 6] provide rich experimental data to this effect). As a result, mechanical characterizations can cover temperatures as low as -80°C but seldom surpass 70°C to 80°C. At higher temperatures, PVB begins to creep or deforms under the force of gravity as it becomes too soft [7]. Therefore, high-temperature characterizations suitable for PVB processing and testing within layered assemblies are difficult to find.

Ref. [7] presents a singular approach for overcoming high-temperature issues with PVB. In here, classical DMA in tension (-40°C to 60°C) was complemented with shear rheometry using a parallel plate configuration (Ø=50 mm, 40°C to 160°C). For the latter part, three 0.76 mm-thick PVB sheets were molten together at 160°C for 30 minutes prior to experimentation. Overall, this particular arrangement led to two distinct sets of constants for the Williams-Landel-Ferry (WLF) law for time-temperature superposition (TTS) and further required assuming full PVB incompressibility to merge the two datasets (Poisson ratio=0.5). Even then, matching of the data was not perfect. Moreover, Ref. [7] acknowledges that achieving TTS in shear rheometry necessitated large vertical shifts (b_T) but does not disclose their relative size. Ultimately, a Prony series including 23 terms was employed to describe the combined data at 20°C, making the description extremely valuable for this reference temperature, but difficult to handle at different ones.

In addition to the absence of a suitable high-temperature description, we have noticed large disparities in the estimates for the long-term (infinite time) elastic response of PVB, viz., E_∞ (or G_∞) when in tension (or shear). From Refs. [4, 5, 6, 8, 9] , we find G_∞ spans $10^3 - 10^5$ Pa, where we assumed $G_\infty = E_\infty/3$ for measurements in tension. It stands to reason that, being an industrial product, the discrepancies may reflect the richness of the PVB family of materials in terms of chemical composition, application, and manufacturer. Yet, Refs. [4, 5, 6] provide comparable G_∞ magnitudes, of about 10^5 Pa, for similar blends coming from two different suppliers (Refs. [4], [5]) and a undisclosed source (Ref. [6]). Consequently, we conclude that PVB is adequately standardized, and accordingly discard PVB variability as a plausible explanation for the size of the disparities. Setting methods aside, a comparison of Ref. [4] (DMA, T_{max} = 70°C, $G_\infty = 1.25\ x\ 10^5$Pa) with Ref. [8] (shear rheometry, T_{max} = 90°C, $G_\infty = 8.0\ x\ 10^3$ Pa) for an identical PVB blend suggests that a high-temperature effect might be at play.

In this paper, we pursued a high-temperature description of polyvinyl butyral. To this end, two PVB sheets were de-aired by vacuum, sealed in an aluminum bag, and further melted together in an autoclave at high temperatures and pressures. We then performed rheological measurements in shear rheometry including both relaxation experiments (step strain) and oscillatory measurements (frequency sweeps). Our results indicate that PVB might behave more like a viscoelastic fluid than the more typical assumption of a viscoelastic solid. We use the theory of reptating chains for entangled melts to show that previous estimates for G_∞ depend on the experiment resolution, in terms of timescale, compared to the reptation time of the polymer chains. Hence, we show that estimates of G_∞stem from imposing an elastic response on an incomplete relaxation. In this respect, comparisons between our results and the data available in the literature bring to light the limitations of existing characterizations when applied to high-temperature situations.

2. Materials & Methods

Herein, we employed a PVB film, in the form of a thin sheet, as classically found within the glass industry. Specifically, the polymer corresponded to RB41 from Eastman. This polymer film is comprised by three monomers, namely, vinylacetate (1-2%wt), vinylalcohol (18-20%wt), and vinylbutyral (80%wt). As detailed in the literature, a plasticizer molecule, namely, triethylene glycol bis (2-ethylhexanoate) is also used in a concentration of about 20-30%wt leading to a $T_g$of around 20°C-30°C [7, 10]. Meanwhile, the film's polydispersity index (PDI) from Size Exclusion Chromatography (SEC) is 1.42 while M_w is ~200 kg mol^{-1} [7]. We verified the PDI and M_w by SEC and found virtually the same results, with a PDI of 1.45 and M_w ~ 219.5 kg mol^{-1}.

PVB materials are highly hygroscopic in nature, with the amount of water dissolved in the bulk dependent on the surrounding atmosphere's relative humidity (% RH). For the blend used here, we measured the uptake of water by Dynamic Vapour Soprtion (DVS) and found it to hold between 0.28-3.1%wt of water in the range of 19.5-91.3% RH. Furthermore, water plays the role of a plasticizer by decreasing the glass transition temperature and reducing the overall observed stiffness in PVB [11, 12]. Thus, we take extra precautions prior to our measurements to ensure a constant amount of water dissolved in the polymer bulk. To this end, all our samples were stored in a climatic chamber, at a nominal relative humidity of 25% before experimentation.

2.1 Sample Preparation

We pursued our experimental characterization in shear rheometry rather than the more classical DMA approach to avoid the previously discussed issues with PVB at high temperatures, to wit, polymer degradation and creeping. The foregoing issues are satisfactory eliminated when working in a parallel plate geometry since adequate contact with the plates can be maintained during the experiment while only exposing the edges of material to the ambient atmosphere. However, a set of issues specific to working with PVB in shear rheometry needed to be overcome. The thin polymer film (approx. 760 µm) displays surface instabilities (sharkskin effect), and, when heated, the film's surface aspect ratio is significantly altered because of the presence of residual stresses. To circumvent these issues, two sheets of PVB were molten together in an autoclave at 140°C and 11 bars of absolute pressure. At this elevated temperature, the polymer is able to fully relax and flow whilst the high pressure guarantees a smooth surface. Preparation wise, the PVB sheets were first sandwiched between two layers of float glass (10 cm x 10 cm x 2 cm), were then subsequently de-aired by vacuum (10 mbar), and were ultimately kept sealed inside an aluminium bag for autoclaving. The PVB sheets were prevented from adhering to the glass by the inclusion of dedicated anti-sticking films. After autoclaving, circular discs (26 mm in diameter) were cut from the final molten smooth layer and served as samples for our

measurements. The discs were then kept in a climatic chamber (25%RH) for a period of 48 hours prior to experimentation.

2.2 Experimental Protocol

For our measurements, we utilized two rheometers, both from Anton Paar, belonging to the series MCR30x running on different software for the acquisition of rheological data. In both rheometers, the samples were heated by means of a Peltier heating system including a heating bottom plate and a passive top disposable plate (25 mm in diameter). The normal force at the top plate was set to zero to maintain adequate contact with the PVB sample. We further utilized a passive hood (solvent trap) to minimize temperature losses to the outside environment. Given the high temperatures surveyed, relative humidity in the rheometers was not controlled. Nevertheless, the aforementioned solvent trap provided some level of atmosphere control. Moreover, considering that only the very thin edges of the samples were exposed during the measurements, we expect minimal amounts of water to escape from the polymer overall. Lastly, a fresh PVB sample was employed each time in all the experiments. In this regard, duplicate runs for each case demonstrated a high level of reproducibility, with minor differences attributed to experimental error.

A MCR301 rheometer was used to perform relaxation experiments whereby we investigated the interlayer response as a function of temperature at a fixed strain. Specifically, we probed the range of 60°C-140°C at a constant strain of $\gamma = 1\%$. Measurements were taken from hot to cold temperatures, starting at 140°C, and decreased afterwards down to 60°C in steps of 20°C. A waiting time of 10 minutes for thermal equilibrium was observed at all temperatures before applying the strain. Finally, we selected the first point of the relaxation at $20t_r$, where t_r is the rise time of the strain (about 0.036 s in our experiments). This time covered both the finite rise time (typical guidelines favour a waiting time of $10t_r$ for step-strain experiments, see Refs. [12, 13]) but also a slight overshoot of the nominal strain, of about 5%-6%, across all temperatures.

A second MCR302 rheometer was employed for oscillatory measurements to determine the master curve of the material in terms of the storage (G') and loss moduli (G''). In this case, we carried out frequency sweeps from 0.1 rad/s to 10 rad/s covering the temperature range of 20°C to 140°C at $\gamma = 0.01\%$. As with the relaxation experiments, measurements were taken from hot to cold temperatures. The same scheme, from high to low, was employed for the application of the frequency. For this experiment, a waiting time of 10 minutes for thermal equilibrium was deemed prohibitive given that the temperature was varied in steps of 5°C. As a result, the oscillating strain was applied automatically by the rheometer whenever the temperature was within 0.5°C of the nominal value. Finally, we performed a temperature sweep ($\gamma = 0.01\%$., $\omega = 1$ rad/s) to quickly determine the glass transition temperature. The T_g was determined using both a Peltier heating system (1°C/min) and a convection oven (1.8°C/min).

3. Results & Discussion

Figure 1 depicts the relaxation modulus of PVB as a function of temperature under constant strain. In general, the interlayer softens dramatically with temperature. To put things into perspective, increasing the temperature from 60°C to 140°C softens the interlayer by roughly three orders of magnitude, from 10^5 Pa to 10^2 Pa, in the timescale of our experiments. Moreover, we note that this very soft state is reached quite rapidly, in the order of 10^2 s, at temperatures common for the processing of PVB (140°C). Contrary to the held assumption of a long-term elastic behaviour, the relaxation curves do not provide evidence towards the existence of a plateau in $G(t)$, let alone one that is temperature dependent. In fact, at all temperatures, $G(t)$ is a monotonically decreasing

function of time. This finding suggests that PVB behaves more like a Maxwell fluid bereft of a long-term elasticity than a solid. In this respect, our results demonstrate that previous estimates for G_∞ are unsuitable in timescales as short as $3x10^2$ s starting at temperatures as low as 100°C.

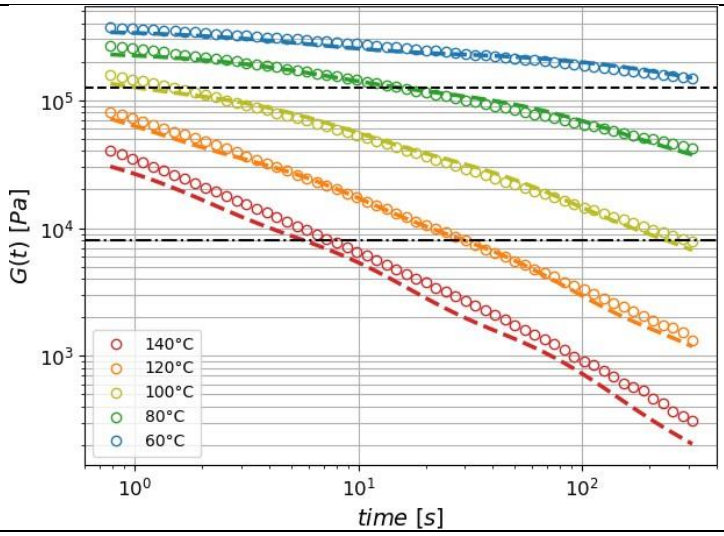

Figure 1: Relaxation modulus for PVB as a function of temperature at $\gamma = 1\%$. Open circles denote experimental data while corresponding coloured dashed lines represent a Generalized Maxwell model with time temperature superposition (Eq. (6)) using the constants from Table 1. *– –, – • – Estimates for G_∞ as found in Refs. [4], [8] for a PVB blend identical to the one used herein.*

Figure 2 shows the time-temperature superposition (TTS) master curve for PVB at 25°C covering 12 decades in the frequency spectrum. The master curve was obtained by exclusive horizontal shifting of the storage and loss moduli curves obtained from oscillatory measurements between 25°C to 140°C. For clarity purposes, we have smoothed the final curves of G', G'', as well as the van Gurp-Palmen plot (top panel in Figure 2), by means of a Savitzky-Golay digital filter. In this way, we preserve the shape of the data, while reducing noise. The latter was predominantly focused on the low frequency (high temperature) region of the dataset. The master curve displays two regions where G', G'' overlap in opposite sides of the frequency spectrum at roughly 10^{-9} rad/s and 1 rad/s, a quasi (rubbery) plateau in G' in between, and a low-frequency region where $G'' \gg G'$. These features are qualitatively in agreement with the findings from Ref. [7] as graphically displayed in Figures 3.8, 3.10 therein. Concerning material parameters, we find the magnitude of the rubbery modulus $G_N^o \approx 3.5x10^5$ Pa from the minimum in between arcs from the van Gurp-Palmen plot as can be seen on the upper left panel of Figure 2. Meanwhile, the horizontal shift factors a_T obey the classical WLF law [14]:

$$\log(a_T) = \frac{-C_1(T - T_r)}{C_2 + T - T_r} \quad (1)$$

where we find $C_1 = 15.32$ and $C_2 = 79.05$°C at $T_r = 25$°C using a non-linear least squares regression.

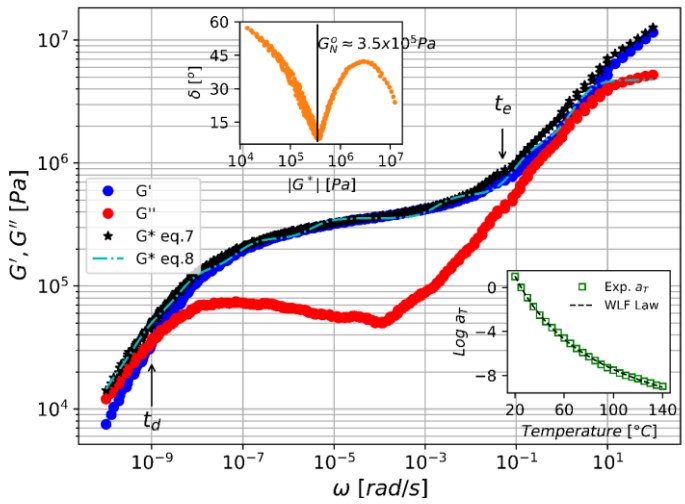

*Figure 2: Time-temperature superposition (TTS) master curve for PVB at 25°C. Top panel: Van Gurp-Palmen diagram, bottom-right panel: Experimental shift coefficients for TTS versus fit of the WLF law (eq. (1)) as a function of the temperature. The curves for G', G'' as well as the Van Gurp-Palmen diagram were smoothed using a Savitzky-Golay digital filter. *Experimental complex modulus G^* (eq. (7)), —•— modelled G^*(eq. (8)).*

The range of application of the WLF law is strictly speaking valid up to $T_g + 100$°C for amorphous polymers [14, 15]. For the PVB herein concerned, we have $T_g \sim 25.5$°C (25 %RH) as given by the peak of the phase angle δ (see Figure 3). Thus, as evidenced by the quality of the WLF law fit on the bottom right panel of Figure 2 (R2 = 0.99), the law remains robust for PVB at least up to $T_g + 115$°C.

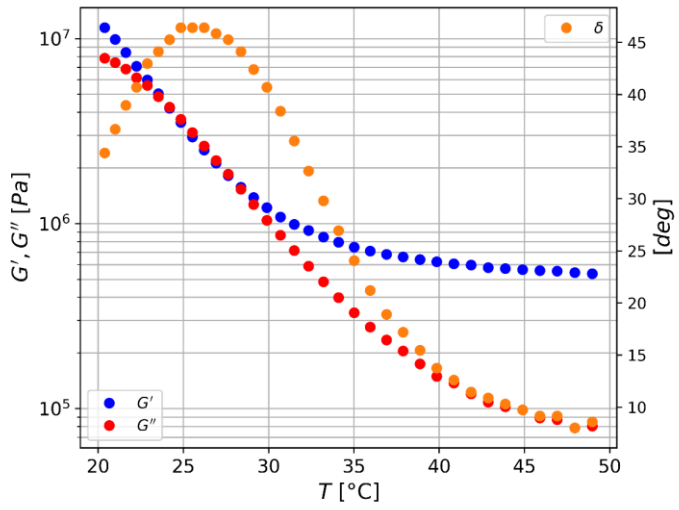

Figure 3: Temperature sweep for PVB, γ =0.01%, ω =1 rad/s, average heating rate 1.8°C/min using a convection oven. A Peltier heater at 1°C/min yielded virtually identical results.

Continuing with the master curve, the shape appears to comply with the Doi & Edwards (DE) theory of entangled chains under small deformation—at least qualitatively. Under this picture, the physical response (not including the glassy state) comprises (1) the relaxation of individual chain links obeying the Rouse model at high frequencies (i.e., a first overlap in G', G'' with $G' \sim \omega^{1/2}$, (2) temporary chain entanglement (reptation) responsible for the quasi-plateau, and (3) viscous flow at low frequencies, were $G'' \gg G'$. All features qualitatively showcased by the PVB master curve. In this treatment, the usage of G_∞ is not necessary, nor does it constitute a material parameter. Equally important, the three aforesaid processes—a priori independent from one another—are separated by two characteristic

times t_e, t_d[1] that are temperature dependent. We show graphically the location of these times in Figure 2, where $t_d \approx 10^9$ s was approximated by the reciprocal of the frequency at the first crossover between G', G'', while $t_d \approx 20$ s, was obtained from eq. (2) [16]:

$$G'(\omega) = G_N^o \sqrt{\frac{\pi}{2}\omega t_e} \text{ for } \omega t_e \gg 1 \quad (2)$$

Roughly speaking, at any temperature T, mechanical solicitations lasting $t < t_e$, will most likely elicit a glassy type of response from PVB. This is the case, for example, for glass assemblies when impacted by a projectile (µs range). For loads lasting $t_e < t < t_d$, the behaviour is largely elastic since the rubbery plateau mandates that $G' \gg G''$. Lastly, when $t > t_d$, PVB enters the melt or viscous state and is capable of flowing. Figure 4 portrays these transitions for a wide range of temperatures and timescales. The illustration, which serves as a type of phase diagram for PVB, utilizes the fact that t_e, t_d, as with any other relaxation time or viscoelastic function, obey TTS [14, 17, 15]. Consequently, when creating Figure 4, it was assumed that:

$$\frac{\omega(T_r)}{\omega(T)} = a_T = \frac{t_e(T)}{t_e(T_r)} = \frac{t_d(T)}{t_d(T_r)} \quad (3)$$

where T and T_r designate an arbitrary temperature and a reference temperature for TTS.

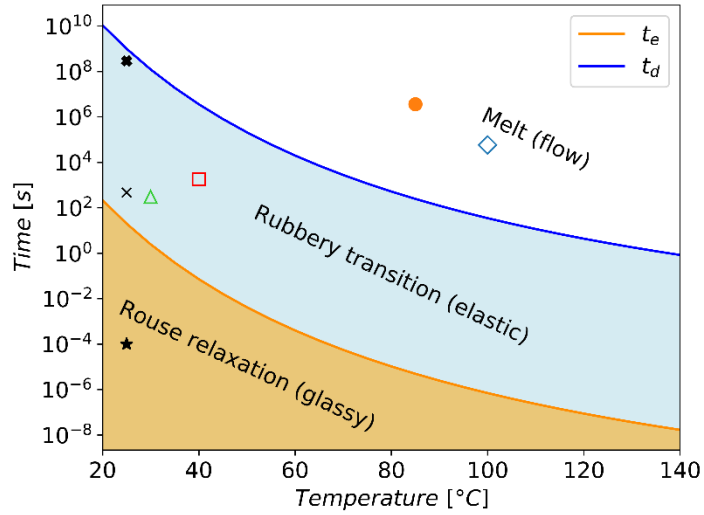

*Figure 4: Time-temperature state diagram for PVB. Solid lines represent the time boundaries between the Rouse relaxation ($t_e \approx 20$ s at 25°C), rubbery plateau, and melt state ($t_d \approx 10^9$ s at 25°C) across the temperature range of 20°C to 140°C using TTS. Markers exemplify the PVB response for different loads: *100 µs ballistic impact at 25°C, ◊Bake tests of safety glass at 100°C for 16 hrs, •Ageing of solar panels at 85°C for 1,000 hrs. Additional time-temperature loads according to international norms from Ref. [18]: □Walking on glass during 30 minutes at 40°C, △Balustrade load, 5 mins at 30°C. [x,x]Total mechanical solicitation from Refs. [4][x], [8][x] as computed in connection with Figure 4. The PVB blend is the same as the one*

[1] Strictly speaking, the DE theory predicts that $t_d = 3Z^3 t_e$, where Z is the number of tube segments. The latter is readily found as $Z = \frac{5}{4} M \frac{G_N^o}{\rho R_u T}$, where M is the molar mass, ρ is the density, R_u is the ideal gas constant, and T is the temperature. The rightmost term in the definition of Z is the reciprocal of the molecular weight between entanglements M_e. For PVB, we find $M_e \sim 7.5\ kg\ mol^{-1}$, with the number of entanglements $M/M_e \sim 26$, and $Z \sim 33$. Taking $t_e \approx 20$ s yields $t_d \approx 2x10^6$ s, thereby falling short of the experimentally observed time $t_d \approx 10^9$s. That the DE theory cannot quantitatively describe the spacing between the characteristic times is hardly surprising since PVB includes three monomers plus a plasticizer molecule, an elevated polydispersity index, and a high level of entanglements. Potentially, a different model may yield a better quantitative matchup. In this respect, given the shape of the master curve, the five-parameter BSW model [20] seems like a suitable candidate. The latter has been used successfully applied to describe other polymeric systems, such as Polystyrene melts and solutions, as seen in Ref. [22]. Nevertheless, a quantitative description of PVB from first principles is beyond the scope of the present work.

used in this work. G_∞, as shown in Figure 1, differs between the refences by approximately an order of magnitude. As depicted in the above diagram, the references also differ in their total solicitation time by roughly five orders of magnitude, with one being deep in the rubbery transition (Ref. [4], $G_\infty = 1.25x10^5$ Pa, T_{max} =70°C), while the other (Ref. [8], $G_\infty = 1.25x10^3$ Pa, T_{max}=90°C) borders the melt state.

The diagram in Figure 4 is extremely useful for understanding the possible transformations PVB can experience during its lifetime. For instance, at room conditions, mechanical solicitations will only evoke two types of response from PVB, viz., the glassy and rubbery states. The melt state, as given by the reptation time, necessitates the passing of decades and is, for all practical purposes, never observed. Interestingly, in this narrow scenario, the rubbery modulus G_N^o is philosophically indistinguishable from a long-term response. By comparison, during a hot summer or heat wave where temperatures may reach peaks of about 50°C, we find from Figure 4, $t_e \approx 4$ ms, and $t_d \approx 2x10^5$ s (or 2.4 days). In this hypothetical case, the glassy state is still perceptible from the perspective of a ballistic impact, but the melt state is now given by a timescale that is relatively short and within the realm of possibility. Thus, under prolonged exposure to high temperatures, PVB's progressive softening and ability to flow could render the foregoing assemblies susceptible to developing optical defects such as bubbles or blisters, or experience delamination. Even further, such assemblies may hypothetically exhibit different performance and failure levels as a function of their geographical location and associated temperatures. For instructive purposes, markers in Figure 4 pinpoint the state/type of response exhibited by PVB for various applications. For instance, typical glass loads, such as those experienced by glass floors (30 mins at 40°C) or balustrades (5 mins at 30°C) [18], elicit a rubbery response from PVB. As a last example, bake/aging tests, as described elsewhere in this paper, force PVB deep into the melt state (see the respective markers in Figure 4).

At this point, we are in a position to address the seemingly disparate estimates for G_∞ found in Refs. [4, 5, 6, 8, 9]. As discussed previously, we do not consider PVB variability as the source of the discrepancies. Rather, we think the issue is linked to a high-temperature effect. For instance, Ref. [5] states that reducing G_∞ is necessary when surpassing temperatures of 40°C to be able to match DMA data with four-point bending tests of glass piles. Aside from the aforementioned engineering considerations, no physical explanation for this reduction was provided. This position, however, is apparently reinforced by Ref. [9] which provides values of G_∞ for -5°C, 20°C, 30°C, and 50°C derived from a combination of weeks-long relaxation/creep tests on double-lap joints with PVB. Setting the glassy state aside, the reported values therein show a decreasing trend with increasing temperature (see the leftmost portion of Figure 5(a)). This softening effect is further supported, as stated earlier, by direct comparison of Refs. [4] and [8].

If the above picture is indeed correct, we would expect to see a marked trend between G_∞ and the maximum experimental temperature used to survey PVB. Nevertheless, as shown in Figure 5(a), this is not the case. Moreover, the existence of a temperature dependent long-term response is contrary to our findings, as well as inconsistent with thermorheological simplicity since PVB is not cross-linked. Instead, we can show that G_∞ in fact comprises a spurious material parameter that is linked to the combined effect of temperature and timescale of experimental observation.

On Figure 5(b), we re-plot the estimates of G_∞ from the literature as a function of the approximate minimum frequency (longest time) achieved in each individual case. To create this figure, we scaled the smallest experimental frequency ω^* by the shift factor a_T^* pertaining to the maximum temperature that was surveyed. In doing so, the effects of time and temperature are simultaneously combined into a single parameter. For measurements in the time domain, we assumed $\omega^* = 1/t_{max}$. Furthermore,

the shift factors for each reference were adjusted to match our reference temperature of 25°C by recomputing the WLF constants via [6]:

$$C_{1,T} = \frac{C_{1,r}C_{2,r}}{C_{2,r} + T - T_r} \quad (4)$$

$$C_{2,T} = C_{2,r} + T - T_r \quad (5)$$

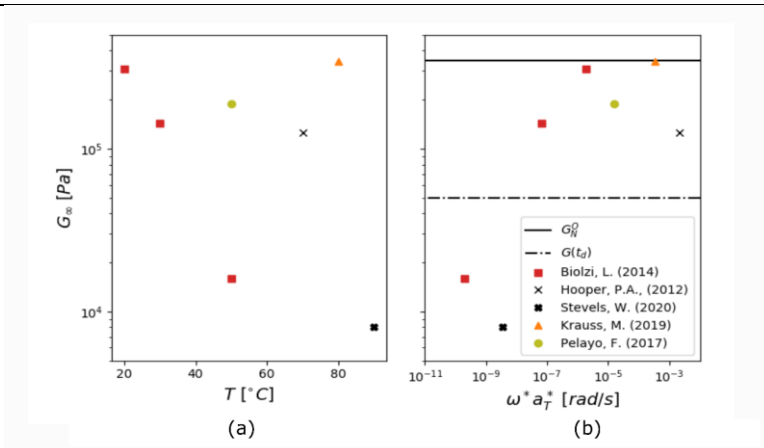

Figure 5: (a): G_∞ estimates from the literature are scattered when plotted as a function of maximum experiment temperature. Figure 5(b): An increasing trend in G_∞ with frequency is revealed when the latter is plotted as a function of minimum frequency as obtained from TTS for a reference temperature of 25°C. Moreover, the data self-categorizes in two regions. A high elasticity region at frequencies $\omega^* a_T^* > \omega_d = 1/t_d \approx 10^{-9}$ rad/s bounded by $G_N^o = 3.5x10^5$ Pa and $G(t_d) \approx 5x10^4$ Pa, as graphically obtained from Figure 2. A low elasticity region, possible influenced by the melt state, is observed when $\omega^* a_T^* \to \omega_d$.

As seen in Figure 4(b), G_∞ values originating from mechanical characterizations spanning a timescale inferior to the reptation time $t \ll t_d$ (or $\omega^* a_T^* \gg \omega_d = 1/t_d \approx 10^{-9}$ rad/s), are accordingly bounded by G_N^o and $G(t_d)$ (the elasticity observed precisely at the time t_d), with the rubbery plateau, G_N^o, giving a clear indication of the order of magnitude for G_∞. Thus, such measurements are strongly influenced by the temporary, yet long-lasting entanglement effect of the polymer chains. Conversely, experiments approaching or exceeding t_d ($\omega^* a_T^* \ll \omega_d$) significantly depart from G_N^o and drop below $G(t_d)$, thereby signalling that the melt state, with an ever-decreasing relaxation, was momentarily reached. Therefore, G_∞, as appraised in the literature, may be the manifestation of numerically forcing a long-term elastic response on two distinct portions of the relaxation, with the unwanted result that disparities occur as a function of the state that was observed. In this respect, we think it is highly unlikely that a specific PVB transformation, such as crosslinking or gelation, may be responsible for some of the values reported for G_∞ in the literature cited here. First, disparities are found when comparing identical PVB blends from the same supplier as a function of experimental conditions as thoroughly discussed above in connections with Refs. [4, 8]. Second, as demonstrated by Ref. [19], unplasticized PVB requires a high level of OH content to transition from amorphous to crystalline (e.g., 63%wt OH). As all the references discussed in the present work involve applications to glass products (i.e., a PVB with a plasticizer molecule), the OH content in such blends—disregarding potentially supplier variabilities or formulations—would nonetheless be much too low to incur in a significant alteration of the PVB physical behaviour [20].

Figure 6 displays the relaxation modulus $G(t)$ for PVB showing simultaneously the Rouse relaxation, rubbery plateau, and melt state. A first part of the relaxation was derived by interconverting the frequency measurements of G', G'' from Figure 2 to the time domain, thereby resolving $G(t)$. This was achieved using Ferry's transformation, i.e., $G(t) = G'(\omega) - 0.4G''(0.40\omega) + 0.014G''(10\omega)\,|_{\omega=1/t}$ [21]. As was the case with Figure 2, we applied a Savitzky-Golay filter to the resulting data to reduce noise. A second part of the relaxation was obtained by shifting the relaxation curves from Figure 1 using the TTS coefficients as obtained from the oscillatory measurements. In here, we added an additional relaxation experiment at 140°C to increase the experimental resolution by an extra decade. As expected from the theory, the datasets formed a single continuous curve without requiring additional adjustments (this was also true when working with the unfiltered oscillatory data). The reference temperature for the relaxation shown in Figure 6 was ultimately shifted to 20°C for ease of comparison with previous references. Lastly, we note that our characterization of the relaxation modulus prioritizes long-timescales. As a result, the glassy state, observed at 20°C for $t < 10^2$ s, and at 100°C for $t < 10^{-7}$ s (see Figure 4), is greatly underestimated. A situation that is exacerbated by the Ferry transformation[2]. Nevertheless, there is extensive data available in the literature on this particular part of the relaxation.

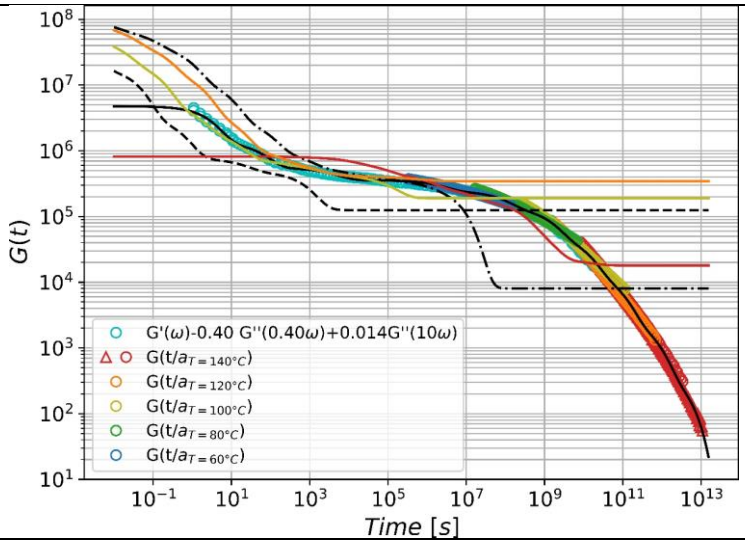

Figure 6: Relaxation curve for PVB at 20°C using TTS. °Interconversion from sinusoidal master curve $G(t) = G'(\omega) - 0.4G''(0.40\omega) + 0.014G''(10\omega)\,|_{\omega=1/t}$ [21]. The signal was smoothed by means of a Savitzky-Golay filter. °ΔRelaxation modulus at 140°C shifted with TTS. °°°Idem for 120°C, 100°C, 80°C, 60°C. – –, – · –, — Maxwell models from Refs. [4], [8] and this work respectively for an identical PVB blend. —,—,— Additional Maxwell models from the literature for other PVB blends or generic PVB designations [5, 6, 9].

Table 1: Elasticity and relaxation times for Maxwell model at $T_r = 25°C$

G_i[Pa]	λ_i[s]	G_i[Pa]	λ_i[s]
3.40E+06	3.34E-01	8.42E+04	1.52E+08
8.09E+05	6.56E+00	3.65E+04	1.23E+09
1.92E+05	4.59E+02	1.14E+04	8.90E+09
1.13E+05	2.56E+05	2.38E+03	6.69E+10
1.08E+05	1.02E+07	4.23E+02	4.84E+11

[2]When using Ferry's approximation, the relaxation modulus G at any time $t = 1/\omega$ is a function of G'' at the shifted frequencies 0.4ω, 10ω. As a result, when interconverting from the frequency space to the time domain, data points on the extremes of the frequency spectrum are lost. For us, this is of little consequence in the small frequency range (long timescale) as the relaxation data far exceeds the frequencies probed. However, some of the long frequency data (short timescale) is invariably lost.

$$G(t,T) = \sum_i G_i \exp\left(\frac{-t}{a_T(T) \times \lambda_i}\right) \quad (6)$$

For simplicity, we describe the relaxation using the Generalized Maxwell model as is standard practice for PVB. Nevertheless, this is slightly modified to include TTS, while excluding G_∞ (eq. (6)). Parameter wise, the model includes 10 Maxwell elements, whose values are summarized in Table 1. The number of elements was determined heuristically, while the constants were obtained by means of a non-linear regression in the log-space using Python 3.0. The model quality across the entire relaxation at 20°C is depicted in Figure 6, while the model's performance at 60°C, 80°C, 100°C, 120°C, and 140°C is shown in Figure 1. Additionally, we show the reliability of the model, as well as the consistency of the relaxation data in the time domain with the measurements in the frequency space, in Figure 2. To this end, we compare the experimental complex modulus G^*given by

$$G^* = G' + jG'' \quad (7)$$

against the corresponding version of eq. (6) in frequency form

$$G^* = \sum_i G_i \frac{\omega^2 \lambda_i^2}{1 + \omega^2 \lambda_i^2} + j \sum_i G_i \frac{\omega \lambda_i}{1 + \omega^2 \lambda_i^2} \quad (8)$$

where j is the imaginary unit, and G_i, λ_i are the spring constants, and relaxation times previously given in Table 1.

Figure 6 additionally provides a comparison between the measurements/model from the present work and those found in the literature. As can be seen, all characterizations, except for Ref. [9], show more or less identical shapes in the Rouse relaxation (for $t < t_e \approx 10^2$ s at 20°C), whilst the timescales differ somewhat. Thereafter, all characterizations reach more or less the same rubbery state (observed roughly between $t_e \approx 10^2$ s $< t < t_d \approx 10^{10}$ s at 20°C), but differ significantly in the terminal flow state, where all, except for the one from this work, saturate at the purported long-time response. Thus, none of the previous characterizations, as previously discussed, are suitable for modelling the transformations undergone by PVB during typical processing conditions. Furthermore, the characterizations from Refs. [4] and [8], which use an identical PVB blend as the one used here, serve as upper and lower bounds for our results in the Rouse transition. Coincidentally, the mechanical description from Ref. [6] for an unknown PVB blend appears to fit perfectly well with our own data in this region. Potentially, the three previous characterizations can be merged with our dataset to increase the resolution of our model deep into the glassy state.

3. Conclusions

By performing relaxation and oscillation measurements in a shear geometry, we explore the rheological response of PVB at high temperature. This allowed us to measure the relaxation modulus as a function of time for different temperatures as well as to construct the master time-temperature superposition curve over a frequency range covering 12 orders of magnitude. This master curve, for which the horizontal shift factors obey the classical WFL law, seems to be in qualitative agreement with the Doi & Edwards theory. In terms of material parameters, we estimated the rubbery modulus $G_N^o \approx 3.5x10^5$ Pa. Meanwhile, the constants for time-temperature superposition where determinised to be $C_1 = 15.32$ and $C_2 =$ 79.05°C ($T_r = 25$°C, range 20°C$< T <$140°C). Likewise, we have

experimentally determined two important characteristic times for PVB, $t_e \approx 20$ s for delineating the glassy/rubbery transition and $t_d \approx 10^9$ s for the rubbery/melt crossover (at 25°C).

By interconverting the frequency measurements in the time scale and shifting the relaxation modulus through the temperature-time superposition, we then obtain the evolution of the relaxation modulus as a function of time over 13 orders of magnitude. This curve, well fitted by a generalized Maxwell model with only 10 Maxwell elements, reveals the predominance of the viscous character of PVB at long times with a vanishing long term elastic modulus. Of course, it is difficult to imagine situations where it would be necessary to know the rheology of PVB at 20°C beyond 10^{10} s (thousands of years). It is less obvious if one is interested in higher temperatures: at 100°C, this viscous state will be reached after $t \approx 100$ s while at 140°C it will be reached after $t \approx 1$ s. This extended analysis of the rheological response of PVB is therefore particularly relevant to understand the appearance of bubbles or defects in PVB confined between two plates at high temperature. This geometry is indeed the one implemented in laminated glass or solar panels, two civil engineering elements designed to last several years and resist high temperatures due to prolonged exposure to the sun or industrial process.

Acknowledgments. We thank Gwennou Coupier, Paul Fourton, Leila Tarhoucht, Diamante Macé, and Rémi Deleurence for their valuable help with the rheology experiments.

Bibliography

[1] C. Carrot, A. Bendaoud, C. Pillon, O. Olabisi and K. Adewale, "Polyvinyl butyral," in *Handbook of Thermoplastics*, Florida, ACRC Press, 2016 , p. 89–138.

[2] M. Kempe, "Modeling of rates of moisture ingress into photovoltaic modules.," *Solar Energy Materials and Solar Cells,* vol. 90, no. 16, p. 2720–2738, 2006.

[3] J. Kapur, K. Proost and C. Smith, "Determination of moisture ingress through various encapsulants in glass/glass laminates," *34th IEEE Photovoltaic Specialists Conference (PVSC),* p. 001210–001214, 2009 .

[4] P. Hooper, B. Blackman and J. Dear, "The mechanical behaviour of poly (vinyl butyral) at different strain magnitudes and strain rates," *Journal of Materials Science ,* vol. 47, no. 8, p. 3564–3576, 2012.

[5] M. Kraus, Machine learning techniques for the material parameter identification of laminated glass in the intact and post-fracture state, PhD thesis, 2019.

[6] F. Pelayo, M. J. Lamela-Rey, M. Muniz-Calvente, M. López-Aenlle, A. Álvarez-Vázquez and A. Fernández-Canteli, "Study of the time-temperature-dependent behaviour of PVB: Application to laminated glass elements," *Thin-Walled Structures,* vol. 119, pp. 324-331, 2017.

[7] P. Elzière, Laminated glass: dynamic rupture of adhesion, PhD thesis, 2016.

[8] W. Stevels and P. D'Haene, "Determination and Verification of PVB Interlayer Modulus Properties," *Challenging Glass Conference Proceedings,* vol. 7, 2020.

[9] L. Biolzi, E. Cagnacci, M. Orlando, L. Piscitelli and G. Rosati, "Long term response of glass–PVB double-lap joints," *Composites Part B: Engineering,* vol. 63, pp. 41-49, 2014.

[10] P. Elzière, P. Fourton, Q. Demassieux, A. Chennevière, C. Dalle-Ferrier, C. Creton, M. Ciccotti and E. Barthel, "Supramolecular structure for large strain dissipation and outstanding impact resistance in polyvinylbutyral," *Macromolecules,* vol. 52, no. 20, pp. 7821-7830, 2019.

[11] M. Desloir, C. Benoit, A. Bendaoud, P. Alcouffe and C. Carrot, "Plasticization of poly (vinyl butyral) by water: Glass transition temperature and mechanical properties," *Journal of Applied Polymer Science,* vol. 136, no. 12, p. 47230, 2019.

[12] M. Botz, K. Wilhelm and G. Siebert, "Experimental investigations on the creep behaviour of PVB under different temperatures and humidity conditions," *Glass Structures & Engineering, ,* vol. 4, no. 3, pp. 389-402, 2019.

[13] V. H. Rolón-Garrido and M. H. Wagner, "The damping function in rheology," *Rheologica Acta,* vol. 48, no. 3, pp. 245-284., 2009.

[14] M. L. Williams, R. F. Landel and J. D. Ferry, "The temperature dependence of relaxation mechanisms in amorphous polymers and other glass-forming liquids," *Journal of the American Chemical society,,* vol. 77, no. 14, pp. 3701-3707, 1955.

[15] C. H. J. Liu and R. B. C. Keunings, "New linearized relation for the universal viscosity-temperature behavior of polymer melts," *Macromolecules,* vol. 39, no. 25, pp. 8867-8869, 2006.

[16] M. Doi and S. F. Edwards, The theory of polymer dynamics, Oxford: Oxford university press., 1988.

[17] C. W. Macosko, Rheology principles. Measurements and Applications, 1994.

[18] W. Stevels, P. D'Haene, P. Zhang and S. Haldeman, " A comparison of different methodologies for PVB interlayer modulus characterization," *Challenging Glass Conference Proceedings,* vol. 5, pp. 399-410, 2016.

[19] M. D. Fernandez, M. J. Fernandez and P. Hoces, "Synthesis of poly (vinyl butyral) s in homogeneous phase and their thermal properties," *Journal of applied polymer science,* vol. 102, no. 5, pp. 5007-5017, 2006.

[20] M. Baumgaertel, A. Schausberger and H. H. Winter, "The relaxation of polymers with linear flexible chains of uniform length," *Rheologica Acta,* vol. 29, no. 5 , pp. 400-408, 1990.

[21] J. D. Ferry, Viscoelastic properties of polymers, John Wiley & Sons, 1980.

[22] Q. Huang, O. Mednova, H. K. Rasmussen, N. J. Alvarez, A. L. Skov, K. Almdal and O. Hassager, "Concentrated polymer solutions are different from melts: Role of entanglement molecular weight," *Macromolecules,* vol. 46, no. 12, pp. 5026-5035, 2013.